mater.scichina.com link.springer.com

Published online 10 October 2023 | https://doi.org/10.1007/s40843-023-2622-1
Sci China Mater 2023, 66(11): 4251–4257

SPECIAL TOPIC: High-performance Structural Materials

Superior fatigue crack growth resistance in bulk Cu with highly oriented nanotwins

Ruike Zhao[1,2†], Huaizhi Zhao[3†] and Lei Lu[1*]

ABSTRACT **We studied the fatigue crack growth (FCG) characteristics of bulk nanotwinned Cu (NT-Cu) with different microstructural aspects such as grain size and twin thickness. We specifically addressed the crack closure, with particular emphasis on the intrinsic FCG resistances in the near-threshold regime. The results demonstrate that the NT-Cu samples have significantly improved fatigue resistances compared with conventional twin-free polycrystalline Cu, a fact we measured using the effective threshold stress intensity factor range, $\Delta K_{th,eff}$. This enhanced resistance can be traced back to the activation of a specific set of primary slip systems in the NT-Cu, known as special *trans*-twin dislocation, which dominates the crack-tip cyclic deformation, leading to a diminished level of cyclical slip irreversibility and, in turn, enhancing the inherent resistance to damage propagation.**

Keywords: nanotwins, fatigue crack growth rate, crack closure, effective crack growth threshold

INTRODUCTION

Most engineering and structural applications would require materials to have a combination of high strength and good ductility, and more importantly, also require materials to have sufficient damage tolerance for safety concerns [1,2]. Unfortunately, these properties are generally mutually exclusive. For example, decreasing grain size down to the nanometer scale induced a significant increase in strength and hardness, while sacrificing the ductility and damage tolerance [3], including fracture toughness and the resistance to subcritical fatigue crack growth (FCG, especially at the near-threshold regime, where the most of the fatigue fracture life is expended).

A series of experiments [4,5] and atomic simulations [6] have shown that the nanoscale growth twins in metals efficiently evade the trade-off between the strength and ductility of metallic materials, where the low-energy coherent twin boundaries (TBs) are effective in blocking dislocation movement and thus substantially strengthen metals, and simultaneously provide plenty of room to store mobile dislocations and contribute considerable ductility [4].

Despite extensive research effort aimed at understanding the strengthening and plastic deformation mechanisms of nanotwinned (NT) metals, there is currently a scarcity of information regarding their damage tolerance characteristics. This knowledge gap primarily arises from the experimental challenges associated with fracture testing at a small scale [7,8]. *In-situ* transmission electron microscopy (TEM) observations on the NT thin films show that the advancing crack can be substantially blunted due to the emission of different types of dislocations from the crack tip [9,10], and the crack growth was hindered by microcrack bridging *via* nanoscale twins [9] or zig-zag fracture paths arising from periodic defections of cracks by TBs [11]. Qualitative fracture toughness measurements based on the contactless video gauging system showed that the fracture resistance of homogeneous NT-Cu is dependent on both the specimen geometry [12] and the microstructural parameters [13]. Furthermore, the embedded nanotwin bundles in the nanograined matrix can also provide significant fracture resistance for the heterostructured sample by triggering anisotropic bridging toughening [14].

To date, only a few experimental studies have been carried out on the FCG behavior of NT metals. Singh *et al.* [15] investigated the FCG characteristic of NT-Cu foils under plane stress conditions, showing that the higher density of nanotwins in a fixed grain size leads to increased resistance to FCG. Alkan *et al.* [16] illustrated that a high volume fraction of TBs contributes to enhanced fatigue damage resistance, a phenomenon directly linked with a reduction in the observed irreversible strain levels at the crack tip. Sangid *et al.* [17] also reported on the superior damage characteristics of NT Ni-Co alloys. Their research provided a logical explanation for these observations, highlighting the influence of nano-scale annealing twins on measured cyclic irreversibility.

Previous studies focusing on NT materials have primarily utilized foil or film samples. Unfortunately, those formats do not facilitate feasible, geometry-independent plane strain FCG testing. Furthermore, the FCG resistance in metallic materials not only stems from the intrinsic factors derived from the inherent microstructural resistance to FCG, but also from the extrinsic aspects caused by crack closure. These extrinsic factors significantly depend on external load conditions [2,18,19], thereby adding further complexity to the determination of inherent

[1] Shenyang National Laboratory for Materials Science, Institute of Metal Research, Chinese Academy of Sciences, Shenyang 110016, China
[2] School of Materials Science and Engineering, University of Science and Technology of China, Shenyang 110016, China
[3] Institute of Fluid Physics, China Academy of Engineering Physics, Mianyang 621999, China
† These authors contributed equally to this work.
* Corresponding author (email: llu@imr.ac.cn)

 © Science China Press 2023

resistance [3,18].

In this study, we aimed to assess the microstructural effects of introducing nanotwins on the inherent resistance to FCG. To do so, we prepared bulk NT-Cu samples by using direct-current electrodeposition, and carefully designed experiments to assess the FCG resistance while taking into account crack closure. In addition, we delved into the mechanisms underlying twin-induced resistance to damage propagation.

EXPERIMENTAL SECTION

Two NT-Cu samples with different grain sizes and twin thicknesses were prepared by direct-current electro-deposition technique at different electrolyte temperatures of 20 and 40°C, respectively. The detailed processing procedures have been described in Ref. [20]. Their cross-sectional microstructures were characterized using back-scattered electrons (BSE) in an FEI Nova NanoSEM 460 scanning electron microscope (SEM).

The specimen geometry and measurement procedure for FCG resistance were based on the recommendation of American Society of Testing Materials (ASTM) Standard E-647 [21]. The compact-tension (CT) specimens with a width, W, of 8 mm, a thickness, B, of 0.5 mm, and an initial notch length, a_0, of 1.6 mm were used in this work. Before testing, the specimen surfaces were ground using silicon carbide paper and polished to a ~0.5-μm mirror finish using the diamond abrasive paste to allow for optical monitoring of the crack length.

Sinusoidal cyclic loading was performed using an Instron E1000 electro-dynamic tester at the constant-amplitude load condition with a frequency of 30 Hz and applied stress ratio, R, of 0.1. The fatigue crack length was continuously monitored by using an optical microscope equipped with a charge coupled device (CCD) image sensor, which provides a high accuracy of up to 0.01 mm. Before the FCG rate test, pre-crack with a length of ~1 mm was introduced under relatively low stress levels and ended with the FCG rate lower than 10^{-10} m per cycle for each specimen. The FCG tests start at a crack length of ~2.6 mm and the initial load range is equal to that at the end of pre-cracking.

FCG rate (crack extension per load cyclic, da/dN) was determined by using the secant method, and the stress-intensity range ($\Delta K = K_{max} - K_{min}$) was calculated according to the ASTM Standard E647 [21]. The FCG curves were plotted as $\log_{10}(da/dN)$ *vs.* $\log_{10}\Delta K$. The fatigue threshold stress-intensity range, ΔK_{th}, was determined as the ΔK value at which the crack growth rate is ~10^{-10} m per cycle.

Crack closure is a critical event that occurs during FCG and is mainly induced by the pre-contact of the upper and lower fracture surfaces during the unloading of the fatigue loading cycle. This phenomenon results in a shift in the slope of load *versus* crack mouth opening displacement (P-v) curves. The points of slope change in these P-v curves can be identified as instances of crake closure [19,22]. The key to identifying these points lies in accurately monitoring the crack mouth opening displacement. In this study, this was achieved using a contactless optical gauging system [13]. Each closure test was documented over several loading cycles at the frequency of 1 Hz. To understand the variation of closure in relation to crack extension, we adopted an experimental measure interval of ~300 μm. The measurement range began at a crack growth rate of ~10^{-10} m per cycle and ended until a catastrophic fracture occurred.

RESULTS

Fig. 1 shows the microstructural characterizations of the NT-Cu

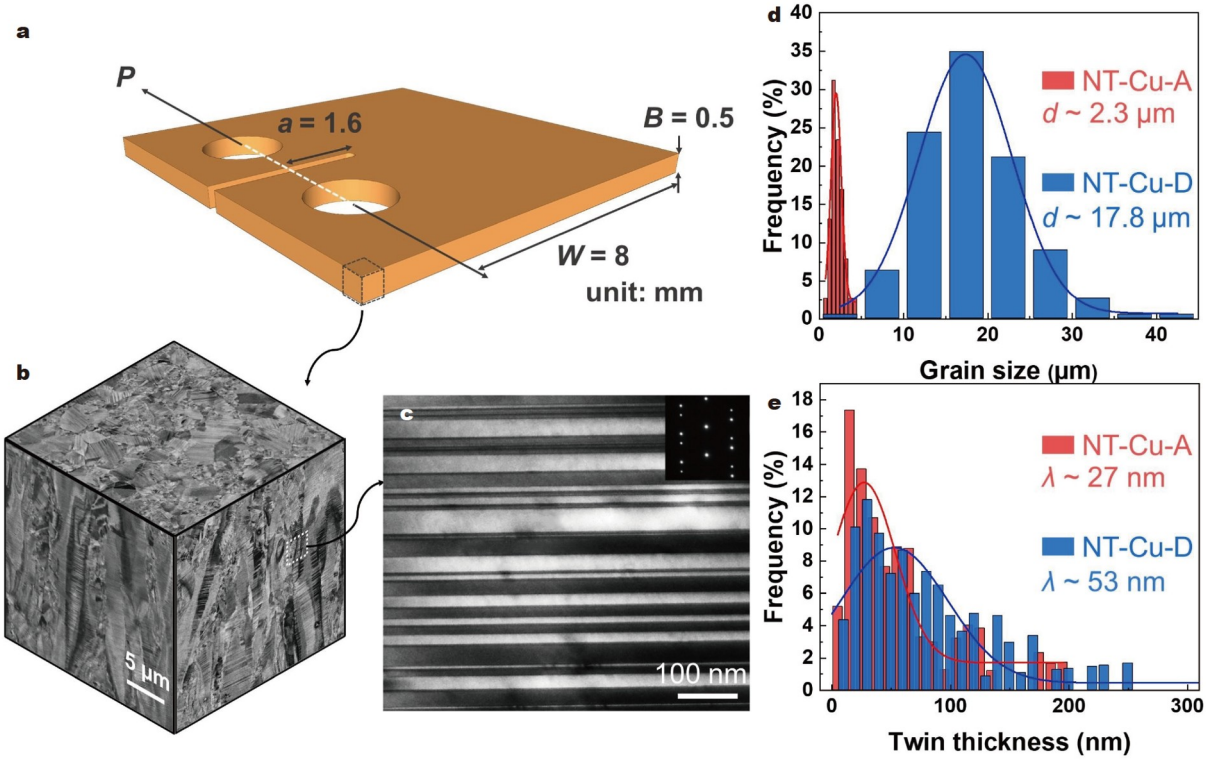

Figure 1 Schematic illustration of the CT specimen (a) and SEM-BSE images projected on a cube to visualize the 3D microstructure of NT-A (b), cross-sectional TEM observation of nanoscale TBs (c). The distributions of grain size (d) and twin thickness (e) of NT-Cu-A and NT-Cu-D.

© Science China Press 2023

samples and the TBs orientation in the CT specimens. The schematic illustration of the CT specimen is shown in Fig. 1a, and the three-dimensional (3D) microstructure of NT-Cu with high densities of parallel growth twin lamellae embedded in columnar grains is shown in Fig. 1b. It is clear that the TBs are predominantly parallel to the electro-deposition growth surface and perpendicular to the crack plane of CT specimens, as indicated in Fig. 1c. A strong (111) out-of-plane texture is detected in the as-deposited Cu samples [20]. Statistical results on the grain size and twin thickness for the two NT-Cu samples are shown in Fig. 1d, e. For consistency with the literature [20,23], we name the samples with smaller average grain size (d = 2.3 μm) and thinner twin thickness (λ = 27 nm) as NT-Cu-A, while the samples with larger average grain size (d = 17.8 μm) and coarser twin thickness (λ = 53 nm) are named as NT-Cu-D. Additionally, a twin-free polycrystalline Cu sample with an average grain size of 20 μm (hereafter referred to as CG-Cu) was also produced for comparison.

Uniaxial tensile tests reveal the average yield strength of NT-Cu-A (σ_{ys} = 436 MPa) is larger than that of NT-Cu-D (σ_{ys} = 238 MPa), but the average uniform elongations turn out to be smaller (1.8% for NT-Cu-A, while 13.7% for NT-Cu-D). The corresponding values of the microstructure characteristics and tensile properties of all samples are summarized in Table 1.

FCG curves of the NT-Cu-A, NT-Cu-D, and CG-Cu samples are shown in Fig. 2 (dashed lines). All the examined curves display a sigmoidal variation and can be categorized into three regimes: (I) near-threshold regime, (II) Paris regime, and (III) unstable regime [1]. A notable difference is evident in the near-threshold regime for the three samples. The FCG threshold (ΔK_{th}), which represents the maximum driving loads for non-growth crack, can be derived from the near-threshold regime. The ΔK_{th} for NT-Cu-D is ~4.91 MPa m$^{1/2}$, which is ~32% higher than that of NT-Cu-A, and ~29% higher than that of CG-Cu (as summarized in Table 1), indicating the introduced nanotwins in larger grains can provide a higher FCG resistance in the near-threshold region.

The FCG in stage II becomes less sensitive to the microstructure, and the FCG behavior in this regime can be described by the Paris Law [24]:

$$da / dN = C(\Delta K)^m. \quad (1)$$

The coefficients C and m are shown in Table 2. It can be seen that the Paris law exponent m of NT-Cu-A (2.7) is considerably smaller than that of NT-Cu-D (5.5) and CG-Cu (6.4), indicating that NT-A exhibits a higher resistance in stage II.

As the crack advanced further into stage III with an increasing ΔK, a rapid catastrophic fracture ensures the following brief stable stage in CG-Cu, as depicted by the black dashed line in Fig. 2. In contrast, the NT-Cu samples exhibit an enhanced fatigue life under stable crack propagation before the ultimately unstable fracture occurs.

To quantify the impact of extrinsic toughening on crack tip shielding, we measured the magnitude of the crack closure. The test method and its foundational logic are schematically illustrated in Fig. 3. It is widely recognized that crack closure is typically triggered by the roughness of the fracture surface and crack-tip plasticity [25], with these effects most noticeable in the

Table 1 Summary of microstructures and mechanical characteristics for NT-Cu-A, NT-Cu-D and CG-Cu[a]

Sample	d (μm)	λ (nm)	σ_{ys} (MPa)	δ_u (%)	ΔK_{th} (MPa m$^{1/2}$)	P_{cl}/P_{max} at threshold $\Delta K_{th,eff}$ (MPa m$^{1/2}$)	
NT-Cu-A	2.3 ± 0.5	27 ± 3	436 ± 10	1.8 ± 0.7	3.33	0.39	2.24
NT-Cu-D	17.8 ± 3.0	53 ± 5	238 ± 8	13.7 ± 1	4.91	0.43	3.10
CG-Cu	20.0 ± 4.0	–	67 ± 5	48.3 ± 1.4	3.81	0.62	1.60

a) d, grain size; λ, twin thickness; σ_{ys}, 0.2% offset yield stress; δ_u, uniform elongation; ΔK_{th}, threshold stress-intensity range; P_{cl}, crack closure load; P_{max}, maximum load; $\Delta K_{th,eff}$, effective threshold stress-intensity range.

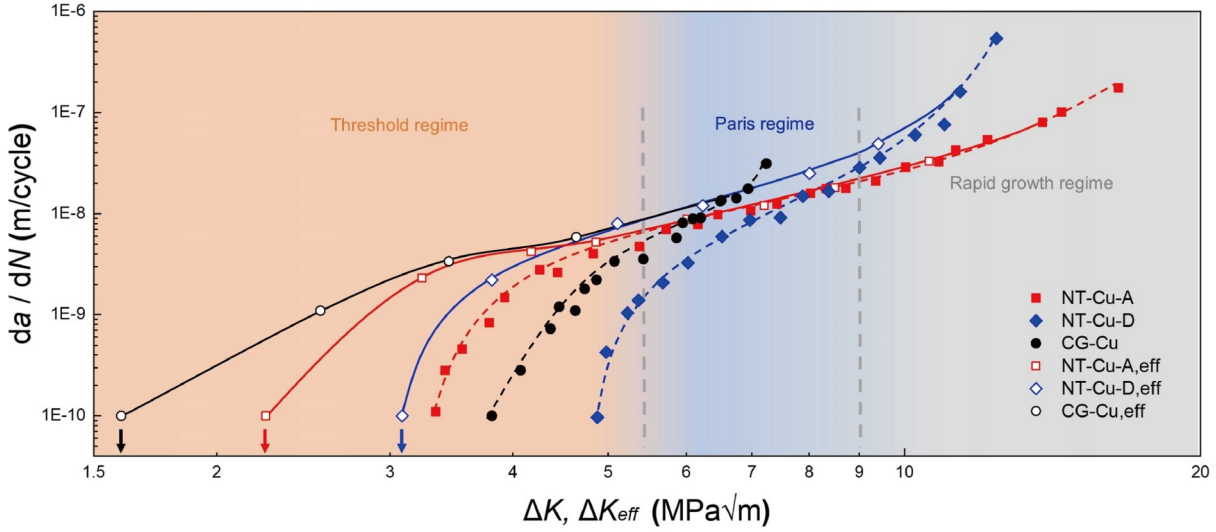

Figure 2 FCG rates, da/dN *versus* ΔK (dashed lines) and ΔK_{eff} (solid lines) of NT-Cu-A, NT-Cu-D and CG-Cu. The arrows indicate the effective crack growth thresholds ($\Delta K_{th,eff}$).

© Science China Press 2023

Table 2 Comparison of the Paris equation constants for the NT-Cu-A, NT-Cu-D and CG-Cu

Samples	C	m
NT-Cu-A	5.0×10^{-11}	2.7
NT-Cu-D	1.6×10^{-13}	5.5
CG-Cu	7.9×10^{-14}	6.4

near-threshold regime. The roughness-induced crack closure predominantly results from a local misfit between the upper and lower fracture surfaces, as shown in Fig. 3b-I. Meanwhile, the plasticity-induced crack closure is thought to be caused by the plastic zone surrounding the wake of the crack tip (Fig. 3b-II) [26–28]. These closure mechanisms cause the crack tip opening displacements (CTODs) to halt prior to the minimum load (P_{min}), thereby shielding the crack tip from a portion to reaching the applied load range [18]. As a result, the effective load range, $\Delta P_{eff} = P_{max} - P_{cl}$, becomes considerably smaller than the initially applied load range ($\Delta P = P_{max} - P_{min}$), which consequently lowers the effective stress intensity factor range ($\Delta K_{eff} = K_{max} - K_{cl}$) at the crack tip below the applied one.

The crack closure loads can be experimentally measured from the P-v curves during the unloading of fatigue loading cycles. Using the NT-Cu-D sample as an example, both local misfit (as shown in Fig. 3b-I) and plastic flow (Fig. 3b-II) can trigger the pre-contact of the fracture surface during the unloading process. As a result, the measured P-v curve (as seen in Fig. 3a) shows a distinct change in slope from the initial unloading stage. The force corresponding to the breaking point in the P-v curve (as indicated by the red circle in Fig. 3a) can be roughly considered as closure load (P_{cl}). In this work, P_{cl} was determined by the intersection of two linear fitted lines adjacent to P_{max} and P_{min}, respectively (as shown by the red and blue lines in Fig. 3a) [22,29].

The ratio of closure load to the maximum load (P_{cl}/P_{max}) is defined to evaluate the degrees of crack closure, and the variation trends of P_{cl}/P_{max} with ΔK in the entire range of the growth rates for the three samples are shown in Fig. 3c. All the curves exhibit larger P_{cl}/P_{max} at the near-threshold region, but the values gradually diminish with increasing ΔK, indicating that the crack-tip shielding induced by crack closure is more prominent in the lower ΔK regimes, where the crack opening displacements (CODs) are relatively small. Furthermore, in the respective near-threshold regime, the coarser-grained samples (CG-Cu and NT-Cu-D) exhibit higher levels of crack closure than the finer-grained NT-Cu-A, which can be attributed to a higher degree of roughness-induced crack closure originating from the rougher fracture surfaces in the coarser-grained materials.

Based on the measurement of P_{cl}/P_{max}, ΔK_{eff} can be derived by using the following formula [25]:

$$\Delta K_{eff} = \Delta K(1 - P_{cl}/P_{max})/(1 - R), \quad (2)$$

where $R = 0.1$ is the load radio. The effective FCG curves (da/dN

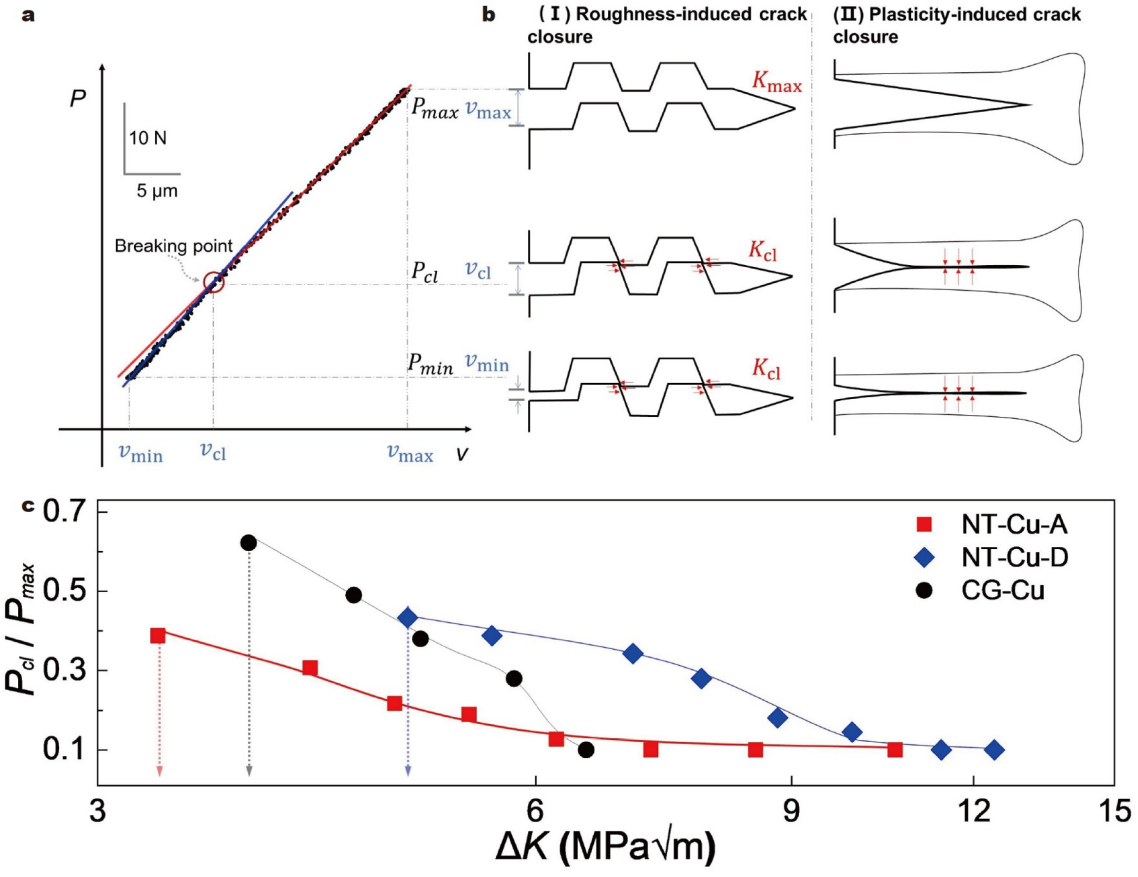

Figure 3 Test method and foundational logic for the measurement of crack closure. (a) P-v curve of NT-Cu-D. (b) Sketch map of two typical mechanisms of crack closure, i.e., (I) roughness- and (II) plasticity-induced crack closure. (c) Variation of the magnitude of crack closure, in terms of the ratio of closure load to the maximum load (P_{cl}/P_{max}), as a function of the stress-intensity range (ΔK). The arrows in (c) indicate the fatigue crack thresholds.

© Science China Press 2023

vs. ΔK_{eff}) on modifying for crack closure are also included in Fig. 2 (solid lines). It is obvious that the effective FCG curves shift to the left compared with their original curves (dashed lines in Fig. 2), particularly in the near-threshold region, where the levels of crack closure are relatively large.

The effective crack growth threshold ($\Delta K_{th,eff}$) can be deemed as an important metric representing intrinsic material resistance to damage propagation at the micro-level, which can be obtained from the da/dN *vs.* ΔK_{eff} curves, as indicated by the arrows in Fig. 2. After excluding the crack closure effect, the $\Delta K_{th,eff}$ values for all the three samples are inevitably reduced compared with their apparent thresholds (ΔK_{th}), but the degrees of reduction are different for NT-Cu and twin-free CG-Cu. For example, the $\Delta K_{th,eff}$ values of NT-Cu-A and NT-Cu-D account for ~67% and ~63% of their respective ΔK_{th}, while that of twin-free CG-Cu is only 42%. More importantly, the $\Delta K_{th,eff}$ value of NT-Cu-D is nearly twice that of the twin-free CG-Cu, though their grain sizes are similar, indicating that the intrinsic microstructural resistance associated with the presence of nanotwins plays a dominant role for the near-threshold damage properties of the NT-Cu samples.

The inherent material resistance to fatigue cracking in the near-threshold regime is a direct consequence of near-tip dislocation slip activities as influenced by the material microstructure [30]. To understand the different FCG behaviors of the NT-Cu and twin-free CG-Cu samples and clarify the different cyclic plastic deformation mechanisms, the crack-tip deformation morphologies in the near-threshold regime and the fracture surfaces in both the near-threshold and Paris regime for the three samples were observed by SEM. As shown in Fig. 4a1 and b1, there is no obvious slip band at the crack tip for both the NT-Cu-A and NT-Cu-D samples. By contrast, numerous slip bands crossed each other are formed around the crack trace in CG-Cu (Fig. 4c1). This suggests that different cyclic slip mechanisms related to fatigue crack propagation are activated in the NT-Cu and CG-Cu samples.

Fracture surface observations show that the NT-Cu-A with finer grains exhibits an intercrystalline-fracture-dominated FCG progress in both the near-threshold regime (Fig. 4a2) and Paris regime (Fig. 4a3), while the NT-Cu-D and CG-Cu with coarser grains show a transition from the mixed intercrystalline and transcrystalline fracture in the near-threshold regime (Fig. 4b2, c2) to the single model of intercrystalline fracture at higher ΔK levels (Fig. 4b3, c3).

DISCUSSION

FCG within the near-threshold regime is primarily through shear modes along the activated slip system; this growth is driven by cyclic slip irreversibility, which enhances the accumulation of local plastic displacement at the tip of the crack [31], causing the crack to extend [15,16,31,32]. For example, a study by Chowdhury *et al.* [30] estimated the effective threshold stress intensity factor ($\Delta K_{th,eff}$) using atomistic simulations. These simulations were centered on the irreversible transfer of discrete

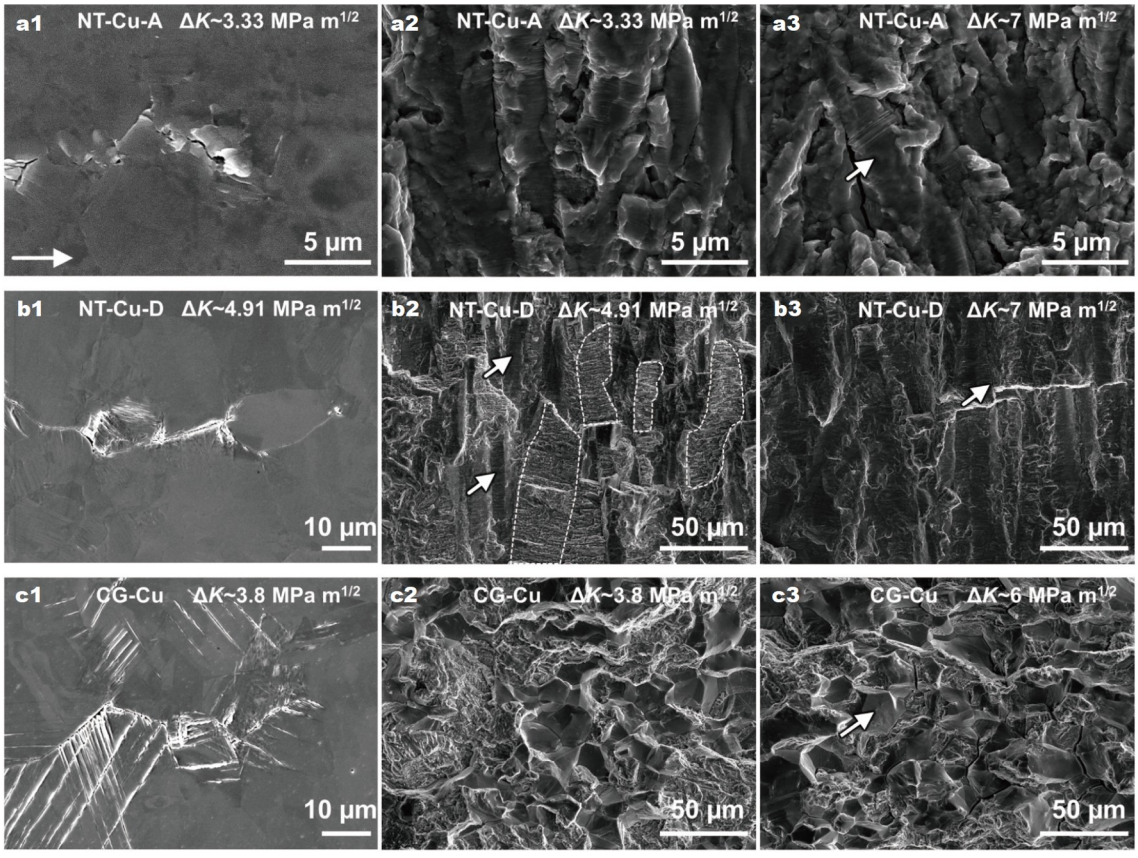

Figure 4 SEM images show the deformation features in the near-threshold regime at fatigue crack tip for the NT-Cu-A (a1), NT-Cu-D (b1) and CG-Cu (c1) samples. Fracture surfaces of the NT-Cu-A (a2 and a3), NT-Cu-D (b2 and b3) and CG-Cu (c2 and c3) samples in both the near-threshold (a2, b2 and c2) and Paris regimes (a3, b3 and c3), respectively. The inset arrow in (a1) indicates the crack growth direction, while arrows in (a3, b2, b3 and c3) indicate the intercrystalline fracture regions. The regions with lamellar morphology which are outlined by dash lines in (b2) indicate transcrystalline fracture.

© Science China Press 2023

dislocations slipping from the crack across TBs, and they found that for relatively short cracks, the fatigue damage resistance improves significantly with the refinement of twin lamellar thickness. This improvement is due to the reduced twin-induced cyclic slip irreversibility caused by the twins at the crack tip as the twin thickness decreases.

The underlying reason for the irreversibility lies in the discrepancies in gliding resistances for dislocations moving forward and backward during the cyclic loading. In the case of CG-Cu, the net irreversibility of dislocation glide trajectories generally derives from diverse dislocation mechanisms, such as mutual annihilation of dislocations with opposite sign [31,32], cross-slipping of screw dislocation [33] and presence of residual dislocations on the cyclical glide paths [34]. As shown in Fig. 4c1, serious damage and cyclic plastic deformation occurred in the crack tip of CG-Cu. This damage is a result of interacting deformation bands that come from the multiple slip systems activated during the cyclic deformation at the crack tip. This leads to an increase in the irreversibility and plastic displacement of the crack tip with each cycle. This, in turn, inevitably speeds up the growth of the crack within the near-threshold regime.

The introduction of nanoscale twins changes the dominating dislocation mechanisms and the total irreversible slip on the glide paths. If we take into account the anisotropic dislocation modes in highly oriented NT-Cu [35] and the orientation relationship between the TBs with crack planes in this work, a single set of primary slip systems will be activated in NT-Cu during the cyclic loading. This group, referred to as special trans-twin dislocations, spans multiple TBs and collectively moves forward and backward along the corrugated {111} slip planes to accommodate the cyclic deformation at the crack tip [35,36].

Importantly, such dislocations are very stable and sustain little resistance from TBs, without any residual dislocation along the cyclical glide paths [36,37], leading to a decrease in the degree of irreversibility. As a result, the damage resistance in the near-threshold regime is increased. As indicated in Fig. 4a1 and b1, there are considerably weaker signs of deformation and less accumulated damage at the crack tip of NT-Cu. The lower levels of irreversible deformation and localized strain are believed to be the reason for higher $\Delta K_{th,eff}$ (Fig. 2).

The FCG resistance of NT-Cu can be improved by adjusting the microstructural parameters. As shown in Fig. 2, both the apparent (dashed lines) and the effective FCG curves (solid lines) show that the near-threshold FCG resistance (in terms of ΔK_{th} or $\Delta K_{th,eff}$) of NT-Cu-D is higher than that of NT-Cu-A, mainly because of their different grain sizes. For NT-Cu-D, the coarser grains create a rough fracture surface, leading to more extrinsic toughening from crack closure (Fig. 3c). Moreover, they reduce the density of the grain boundary (GB) within the cyclic plastic zone at the crack tip. These GBs usually act as the barriers, resulting in irreversible glide trajectories and also serving directly as the pathway for crack growth, leading to the dominated intercrystalline fracture in NT-Cu-A (Fig. 4a2, a3).

However, with gradually increasing ΔK into the Paris regime, the FCG resistance of NT-Cu-A becomes larger than that of NT-Cu-D (as indicated by the lower m value for NT-Cu-A). In this stage, the FCG rate is considered to be proportional to the CTOD [1]. The higher yield strength in NT-Cu-A, originating from the refined twin thickness and the grain size, leads to a lower CTOD and thus a decreased FCG rate, making NT-Cu-A prevail in stage II.

Understanding the impact of individual parameters like grain size and twin thickness on the FCG resistance of NT-Cu is crucial. It provides important insights into how we can design an optimized microstructure for maximum damage tolerance. Due to the strong coupling between these two microstructural features during the preparation of NT-Cu, it is impossible to achieve this goal in the present work. Still, both the experimental [15–17] and simulation [30,34,38] studies have suggested that refining the twin thickness can substantially improve the FCG resistance of NT materials. Given the current experimental results in this work, it makes sense to say that introducing a higher density of nanotwins into the larger grains could further enhance the FCG resistance in both stages I and II. To further verify the mechanisms of cyclic deformation at the crack tip and measure the slip irreversibility at the crack tip of NT-Cu, we need in-depth investigations using *in-situ* electron microscopy investigations and atomistic simulations.

CONCLUSIONS

In summary, we studied the intrinsic FCG behavior of NT-Cu with different grain sizes and twin thicknesses by considering their impact on crack closure. The results demonstrate that the intrinsic FCG resistances of NT-Cu in the near-threshold regime (as indicated by the measured $\Delta K_{th,eff}$ levels) are significantly higher than that of conventional twin-free polycrystalline Cu. This improvement is primarily due to the activation of the special trans-twin dislocations during the cyclic deformation at the crack tip in NT-Cu. This action leads to a reduced level of irreversibility, and as a result, the damage resistance is increased accordingly. These results advance our fundamental understanding of the FCG resistance of materials with nanotwins, and insight into the design of new damage-tolerant structure materials.

Received 5 August 2023; accepted 18 September 2023; published online 10 October 2023

1 Suresh S. Fatigue of Materials (2nd edition). Cambridge: Cambridge University Press, 1998
2 Ritchie RO. Mechanisms of fatigue-crack propagation in ductile and brittle solids. Int J Fract, 1999, 100: 55–83
3 Hanlon T, Tabachnikova E, Suresh S. Fatigue behavior of nanocrystalline metals and alloys. Int J Fatigue, 2005, 27: 1147–1158
4 Lu L, Chen X, Huang X, *et al.* Revealing the maximum strength in nanotwinned copper. Science, 2009, 323: 607–610
5 Shen YF, Lu L, Lu QH, *et al.* Tensile properties of copper with nanoscale twins. Scripta Mater, 2005, 52: 989–994
6 Li X, Wei Y, Lu L, *et al.* Dislocation nucleation governed softening and maximum strength in nano-twinned metals. Nature, 2010, 464: 877–880
7 Zhao H, Li Z, Gao H, *et al.* Fracture and toughening mechanisms in nanotwinned and nanolayered materials. MRS Bull, 2022, 47: 839–847
8 Lu L, Zhao HZ. Progress in strengthening and toughening mechanisms of heterogeneous nanostructured metals. Acta Metall Sin, 2022, 58: 1360–1370
9 Kim SW, Li X, Gao H, *et al. In situ* observations of crack arrest and bridging by nanoscale twins in copper thin films. Acta Mater, 2012, 60: 2959–2972
10 Liu L, Wang J, Gong SK, *et al.* Atomistic observation of a crack tip approaching coherent twin boundaries. Sci Rep, 2014, 4: 4397
11 Shan ZW, Lu L, Minor AM, *et al.* The effect of twin plane spacing on the deformation of copper containing a high density of growth twins. JOM, 2008, 60: 71–74

 © Science China Press 2023

12 Luo S, You Z, Lu L. Thickness effect on fracture behavior of columnar-grained Cu with preferentially oriented nanoscale twins. J Mater Res, 2017, 32: 4554–4562
13 You Z, Qu S, Luo S, *et al.* Fracture toughness evaluation of nano-structured metals *via* a contactless crack opening displacement gauge. Materialia, 2019, 7: 100430
14 Zhao HZ, You ZS, Tao NR, *et al.* Anisotropic toughening of nanotwin bundles in the heterogeneous nanostructured Cu. Acta Mater, 2022, 228: 117748
15 Singh A, Tang L, Dao M, *et al.* Fracture toughness and fatigue crack growth characteristics of nanotwinned copper. Acta Mater, 2011, 59: 2437–2446
16 Alkan S, Chowdhury P, Sehitoglu H, *et al.* Role of nanotwins on fatigue crack growth resistance—Experiments and theory. Int J Fatigue, 2016, 84: 28–39
17 Sangid MD, Pataky GJ, Sehitoglu H, *et al.* Superior fatigue crack growth resistance, irreversibility, and fatigue crack growth–microstructure relationship of nanocrystalline alloys. Acta Mater, 2011, 59: 7340–7355
18 Ritchie RO. Mechanisms of fatigue crack propagation in metals, ceramics and composites: Role of crack tip shielding. Mater Sci Eng-A, 1988, 103: 15–28
19 Gan D, Weertman J. Crack closure and crack propagation rates in 7050 aluminum. Eng Fract Mech, 1981, 15: 87–106
20 Cheng Z, Zhou H, Lu Q, *et al.* Extra strengthening and work hardening in gradient nanotwinned metals. Science, 2018, 362: eaau1925
21 Standard Test Method for Measurement of Fatigue Crack Growth Rates. American Society of Testing and Materials, 2015
22 Rackwitz J, Yu Q, Yang Y, *et al.* Effects of cryogenic temperature and grain size on fatigue-crack propagation in the medium-entropy CrCoNi alloy. Acta Mater, 2020, 200: 351–365
23 You ZS, Lu L, Lu K. Tensile behavior of columnar grained Cu with preferentially oriented nanoscale twins. Acta Mater, 2011, 59: 6927–6937
24 Paris P, Erdogan F. A critical analysis of crack propagation laws. J Basic Eng, 1963, 85: 528–533
25 Pippan R, Hohenwarter A. Fatigue crack closure: A review of the physical phenomena. Fatigue Fract Engng Mater Struct, 2017, 40: 471–495
26 Suresh S, Ritchie RO. A geometric model for fatigue crack closure induced by fracture surface roughness. Metall Trans A, 1982, 13: 1627–1631
27 Riemelmoser FO, Pippan R. Crack closure: A concept of fatigue crack growth under examination. Fatigue Fract Eng Mater Struct, 1997, 20: 1529–1540
28 Wolf E. Fatigue crack closure under cyclic tension. Eng Fract Mech, 1970, 2: 37–45
29 Liaw PK, Leax TR, Williams RS, *et al.* Near-threshold fatigue crack growth behavior in copper. Metall Trans A, 1982, 13: 1607–1618
30 Chowdhury PB, Sehitoglu H, Rateick RG. Predicting fatigue resistance of nano-twinned materials: Part II—Effective threshold stress intensity factor range. Int J Fatigue, 2014, 68: 292–301
31 Pippan R. Dislocation emission and fatigue crack growth threshold. Acta Metall Mater, 1991, 39: 255–262
32 Pippan R. The condition for the cyclic plastic deformation of the crack tip: The influence of dislocation obstacles. Int J Fract, 1992, 58: 305–318
33 Mughrabi H. Cyclic slip irreversibility and fatigue life: A microstructure-based analysis. Acta Mater, 2013, 61: 1197–1203
34 Chowdhury PB, Sehitoglu H, Rateick RG. Predicting fatigue resistance of nano-twinned materials: Part I—Role of cyclic slip irreversibility and Peierls stress. Int J Fatigue, 2014, 68: 277–291
35 You Z, Li X, Gui L, *et al.* Plastic anisotropy and associated deformation mechanisms in nanotwinned metals. Acta Mater, 2013, 61: 217–227
36 Bu L, Cheng Z, Zhang Y, *et al.* Trans-twin dislocations in nanotwinned metals. Scripta Mater, 2023, 229: 115348
37 Pan Q, Zhou H, Lu Q, *et al.* History-independent cyclic response of nanotwinned metals. Nature, 2017, 551: 214–217
38 Chowdhury PB, Sehitoglu H, Rateick RG, *et al.* Modeling fatigue crack growth resistance of nanocrystalline alloys. Acta Mater, 2013, 61: 2531–2547

Acknowledgements Lu L acknowledges the financial support by the National Natural Science Foundation of China (NSFC, 51931010 and 92163202) and the Key Research Program of Frontier Science and International partnership program (GJHZ2029).

Author contributions Lu L designed and supervised the project; Zhao R and Zhao H performed the experiments. All authors analyzed the data, discussed the results and wrote the paper.

Conflict of interest The authors declare that they have no conflict of interest.

Ruike Zhao is currently a PhD student under the supervision of Professor Lei Lu at the Institute of Metal Research, Chinese Academy of Sciences (CAS), China. He received his Bachelor degree from Northeastern University, China, in 2019.

Huaizhi Zhao received his PhD degree in materials physics and chemistry from the University of Science and Technology of China in 2022. He is currently a research scientist at the Institute of Fluid Physics, China Academy of Engineering Physics. His research focuses on the deformation and fracture behavior of bulk nanostructured metallic materials.

Lei Lu is a distinguished professor at Shenyang National Laboratory for Materials Science at Institute of Metal Research, CAS, China. Her research interests include the synthesis, microstructure design and characterization, plastic deformation, and mechanisms of heterogeneous nanostructured metallic materials. She is an editor for *Acta Materialia* and *Scripta Materialia,* and an associate editor for *Science China Materials*.

块体择优取向纳米孪晶铜的优异抗疲劳裂纹扩展性能

赵瑞珂[1,2†], 赵怀智[3†], 卢磊[1*]

摘要 本文研究了具有不同微观结构(如晶粒尺寸和孪晶厚度)的块体择优取向纳米孪晶Cu(NT-Cu)的疲劳裂纹扩展(FCG)特性, 着重讨论了裂纹闭合效应和近门槛值区域的本征FCG阻力. 与传统无孪晶的粗晶Cu相比, NT-Cu样品表现出显著提升的疲劳裂纹扩展抗力(有效门槛值应力强度因子范围, $\Delta K_{th,eff}$). 这种增强的裂纹扩展阻力与NT-Cu中特殊的跨孪晶位错滑移模式有关. 该位错主导着NT-Cu裂纹尖端的循环变形, 有效降低了裂纹尖端循环滑移不可逆水平, 从而提高了纳米孪晶材料损伤扩展的本征抗力.

 © Science China Press 2023